

Influence of aqueous chloride and bromide anions on the reactivity of ZnO on bisphenol A degradation

Yi-Chen Yang

National Taiwan University

Rama Shanker Sahu

National Taiwan University

Yang-hsin Shih (✉ yhs@ntu.edu.tw)

National Taiwan University <https://orcid.org/0000-0002-1326-0720>

Research

Keywords: BPA, Zinc oxide (ZnO), Photodegradation, Electrolyte, Hydrodynamic particle size

Posted Date: May 6th, 2021

DOI: <https://doi.org/10.21203/rs.3.rs-421019/v1>

License: © ⓘ This work is licensed under a Creative Commons Attribution 4.0 International License.

[Read Full License](#)

Abstract

Zinc oxide nanoparticles (ZnO NPs) have been widely investigated for applications in photocatalytic degradation of organic pollutants in wastewater. Despite the advantages of robust ZnO material, its photocatalytic activity is greatly affected by environmental factors. Halogen ions are commonly found in wastewater, which directly affect the pollutant aggregation and sedimentation, therefore it is necessary to discuss their effect on the photodegradation. The current study assesses the halogen ions effect on the photocatalytic degradation of bisphenol A (BPA) using different dosage of sodium chloride (NaCl) and sodium bromide (NaBr). The microstructural characterization of ZnO was conducted by transmission electron microscopy and hydrodynamic size was analyzed through dynamic light scattering. Degradation reactions of BPA with ZnO NPs followed pseudo-first-order kinetics. The increase of ZnO dosage from 0.01 g/L to 0.1 g/L enhanced the degradation rate constant of BPA up to 0.089 min^{-1} (14.8 folds). In order to evaluate the the role halogen ions to degrade BPA, NaBr and NaCl were used. The degradation rate was reduced up to 26 folds (0.0034 min^{-1}) after the addition of NaBr, which was attributed to the increase in hydrodynamic particle size leading, thereby restricting the light adsorption capacity. Noteworthy, upon addition of NaCl from 10 mM to 500 mM concentration, there was only a slight decrease (2.4 folds, 0.037 min^{-1}) on the degradation rate of BPA. Therefore, this study unveils the role of chloride ions as an effective medium for BPA degradation by ZnO NPs, without aggregation, and provides a novel platform for the treatment of organic pollutants in saline water.

1. Introduction

World-wide contamination of phenolic compounds in aquatic environmental has attracted increasing attentions in the research society. Bisphenol A (BPA) used as basic monomer in the synthesis of brominated flame retardants, epoxy resins and polycarbonates due to which it became the highest produced chemical worldwide [1]. However, their characteristics, environmental distribution and adverse effect on human health remain less-known compared to conventional pollutants, the worldwide demand is dramatically increasing [2]. BPA is one of the endocrine disruptors due to its genotoxic and estrogenic activity, which damage the reproduction and brain development [3]. Owing to the discharge of wastewater and improper accumulation of solid waste, BPA has been ubiquitous in the world [4]. In some rivers, BPA concentration could even reach up to $8 \mu\text{g/L}$ [5], and the report from Barboza et al. also revealed the present of BPA and its analogs in muscle and liver of fish [6]. In China, up to 144 ng/mL of bisphenol analogues was detected in serum samples from pregnant women [7]. Since even low concentration of BPA causes hazardous health, the development of treatment techniques with efficiency is required.

Treatment of contaminated wastewater has received increasing attention. Several techniques such as chemical oxidation [8], sono-photo-Fenton oxidation [9], UV-assisted chemical oxidation [10], electrochemical degradation [11], nano zerovalent iron (NZVI) reduction [12], biodegradation [13] and adsorption methods [14] were studied. Chemical oxidation is widely used for wastewater treatment, such as Fenton process [15] and ozone treatment [16] could effectively oxidize the organic contaminants in the

aquatic system. Electrochemical method [11] is to apply electrolysis for contaminant removal. NZVI has appropriate redox potential to reduce organic contaminant under anaerobic conditions but cannot totally mineralize contaminant structures because it tends to lose reducing activity due to easy oxidation in the air. Previous studies reported that BPA is biodegradable by bacterial strains [17], while it takes at least several days to remove BPA and produces byproducts. Activated carbon is commonly used for adsorption of compounds in air or aquatic system and the adsorption capacity depends on the carbon used and the characteristic of wastewater [18, 19]. However, physical adsorption is cost effective treatment procedure but generate huge wastage, which requires further treatment. Various studies suggest that chemical reduction, advanced oxidation and electrochemical processes are desired and effective treatment procedure for BPA, which could be activated by using expensive and noble metal catalysts [20]. Silver nanoparticle (NPs) activation by hydrogen peroxide system was used for photocatalytic degradation of BPA [21]. However, enhanced BPA removal was reported but presence of H_2O_2 can quickly dissolve silver nanoparticles in the solution, therefore polyvinyl alcohol was further immobilized to stabilize the nanoparticle. Moreover, NZVI has been exploited in last 4 decades for waste water treatment but agglomeration due to intrinsic magnetic properties and quick aerial oxidation of NZVI remain the major challenges [22].

The natural phenomenon involves the direct photodegradation of organic chemicals in the environment. The addition of photocatalysts influence the degradation efficacy as well as complete mineralization of organic pollutants. In this regard, ZnO environmentally benign material has been used for photocatalytic oxidation of pollutants. ZnO is attractive to be used in photodegradation since its non-toxicity, great optical properties, and relatively low cost [23]. The commercial or chemically modified ZnO NPs have demonstrated substantial differences in their morphology, shape and size, and photoelectric properties which show important role in the optical properties and photoactivity of ZnO NPs. However, previous studies showed that the effect of environmental factors such as pH, electrolytes and organic compounds are important and needed to be considered in the ZnO photodegradation process. It was observed that the adsorption of the dyes onto the surface of ZnO NPs is strongly influenced by the pH of the solution since the surface charge of both NPs and contaminants change at different pH values [24]. The effect of electrolytes on ZnO photodegradation has been widely reported, while whether the addition of electrolytes can increase or decrease degradation efficiency is still unsure in different conditions. Lee et al. [25] demonstrated the role of various inorganic species such as BrO_3^- , $S_2O_8^{2-}$ and SO_3^- could be advantageous to enhance the photodegradation of organic contaminants in the presence of ZnO NPs. However, some inorganic ions such as Cl^- , NO_3^- and CO_3^{2-} will tend to retard the photodegradation of ZnO. It is obvious that electrolytes existing in wastewater will pose a challenge for photocatalyst treatment. Therefore, an understanding performance of ZnO photocatalyst in existence of electrolytes is crucial for assessing the feasibility of ZnO photodegradation in the practical application.

The current study demonstrates the effect of electrolytes on the photodegradation of BPA, one of environmental endocrine disruptor using ZnO NPs under UV light irradiation. The effect of ZnO dosages on photocatalytic degradation of BPA was investigated to optimize the optimum catalyst dose. The

experiments under the influence of different electrolyte concentrations (NaCl and NaBr) were performed and the change in hydrodynamic particle sizes were also monitored. The relationship among electrolyte concentration, ZnO particle size and reaction kinetics is discussed.

2. Materials And Methods

2.1 Materials

The commercial powder zinc oxide (Uniregion Biotech) with particle size of 20 nm was used in the experiments. Bisphenol A (CAS No. 80-05-7), sodium chloride and sodium bromide in this research were obtained from Acros Organics. All solutions were prepared with ultrapure water.

2.2 Characterization of ZnO analysis

The morphology of ZnO NPs was analyzed by transmission electron microscopy (TEM). NPs suspensions were prepared by adjusting to appropriate concentrations at room temperature under ultrasonication for 10 min. In aqueous systems, particle size of photocatalysts and their distributions were measured by a dynamic light scattering (DLS) instrument (Zetasizer nano ZS, Malvern nano series V6.0). UV-vis spectra was used to record the light absorption property of ZnO nanoparticle under the wavelength between 200 nm to 800 nm. The sedimentation of those large agglomerates of ZnO NPs was also monitored with UV-vis spectra at 365 nm in 90 minutes. High performance liquid chromatography (HPLC, Agilent 1200 series) equipped with C-18 column, auto-injector, and variable wavelength detector was used to analyze the concentration of BPA in the experiments.

2.3 Photodegradation experiments

The typical photocatalytic experiments were conducted in the laboratory. A photochemical reactor was equipped with four 8-W UV lamps at the irradiation wavelength of 365 nm. Experimental solutions in tubes were placed in a rotor inside the photochemical reactor to irradiate them equally. In degradation experiments, a solution that contained different ZnO NPs photocatalyst dosages and 5 ppm BPA was prepared to conduct the experiments. After 30-minutes dark adsorption experiment, the solutions were illuminated under the light at the irradiation wavelength of 365 nm. During the experiment, the aliquot of 2 mL was collected, filtered through 0.22-micron filter and the concentration of BPA was analyzed by HPLC through auto-injector at selected intervals.

2.4 Chloride and bromide ions effect

NaCl and NaBr were used as electrolyte under specific dosage of ZnO to evaluate BPA degradation in the following experiments. The concentration of chloride or bromide ranged from 0 mg/L to 500 mg/L. Before performing the experiments, the electrolyte and ZnO was added to the solution containing 5 ppm BPA, stirred for 1 minute and kept in the dark for 30 minutes to attain adsorption and desorption equilibrium before the photodegradation. The aliquot of 2 mL was collected, filtered through 0.22-micron

filter and analyzed by HPLC through auto-injector at desired intervals. DLS and pH analysis were also carried out after every batch of experiment.

3. Result And Discussion

3.1 Morphological characterization of ZnO NPs

The morphology of ZnO NPs was first analyzed by TEM. Fig. 1a shows that the particle sizes of ZnO NPs are homogenously distributed in the range of 35 nm. However, due to the high surface potentials of NPs, ZnO NPs aggregate in storage and need dispersion before the usage in experiments. NPs aggregate to form big agglomerates and the particle sizes can approach microscale, when suspended in DI water. ZnO NPs aggregation was further analyzed by DLS (Fig. 1b), depicts the average nanoparticle size of ZnO in water is about 250 nm after sonification. Many studies applied ultrasonication to suspend NPs in aqueous solution before experiments [26]. Therefore, ZnO suspensions used in experiments was allowed for 30 minutes ultrasonication in advance to properly disperse NPs. The full-scale UV-visible spectra of ZnO NPs was obtained and depicted in fig. 1c to confirm the light absorption range (365 nm), which is corresponding to a broad band gap (3.39eV) in Choi et. al.'s report [27].

3.2 Photodegradation of BPA

The photocatalytic degradation of 5 ppm BPA was performed by varying the dosage of ZnO from 0.01 to 0.1 g/L under 365 nm UV light (Fig. 2a). The degradation rate constants (k) were determined by a pseudo-first-order rate kinetics [28]:

$$C = C_0 e^{-kt}$$

where C is the concentration of BPA after time t , C_0 is the initial concentration of BPA, t is the reaction time, and k is the pseudo-first-order rate kinetics.

The photocatalytic degradation rate can be properly described by pseudo-first-order kinetics under different ZnO dosages. Enhanced rate of BPA was observed when ZnO NPs dose increased from 10 mg L⁻¹ to 100 mg L⁻¹ (0.006 min⁻¹ to 0.089 min⁻¹). Previous studies also indicated that photocatalytic degradation rates of NPs on organic contaminants can be described by pseudo-first-order kinetics [29, 30]. The enhancement of the degradation rate of BPA was observed with the increase of ZnO dosage from 0.01 to 0.1 g/L, owing to the increase in the concentration of catalyst and adsorption sites on ZnO surface. The result of full scan also showed that the fraction of UV light absorbed by the catalyst increased as the concentration of ZnO increased in a suspension (Fig. 2b). Therefore, 100 mg/L ZnO NPs catalyst dose was used during entire photocatalytic experiments. Previous studies indicate that OH radicals and positive holes play the major role in ZnO photodegradation process [31, 32]. Owing to the increased yield of OH radicals as the dosage of ZnO increased, the proportion of reactive oxygen species that attack BPA and its intermediates increases. There was no significant adsorption was observed when

the dosage of ZnO was 0.02, 0.05 and 0.1 g/L, while the removal of 7% BPA by 0.1 g/L ZnO was observed in the first 30 minutes under dark condition. Considering of economic efficiency, the following experiments were performed with the dosage of 0.02 g/L ZnO.

3.3 The effect of sodium chloride on photodegradation of BPA

The effect of different NaCl concentration on the photocatalytic degradation performances of ZnO on BPA was evaluated (Fig. 3). Fig. 3a shows the increase of NaCl concentration in the reaction resulting in slower BPA removal, except that degradation rate constant was decreased around 50 % by 500 mM NaCl. The BPA rate constants were calculated 0.089, 0.038, 0.035 and 0.032 min⁻¹ for 0 mM, 10 mM, 100 mM and 500 mM NaCl, respectively (Fig. 3b). The Previous studies reported that in the presence of electrolytes, the compression of the electrostatic double layer of NPs occurs, causing particle aggregation, decrease of surface area and therefore the decline of the photocatalytic degradation activity [33, 34]. The effect of NaCl on ZnO NPs was investigated and observed the absorbance change over time. The average hydrodynamic particle size of ZnO NPs after degradation experiments were determined by UV-visible spectra and DLS, respectively. It was observed that the absorbance of ZnO NPs without NaCl decreased 17%. The absorbance decreased up to 32% with 500 mM NaCl concentration after 90 minutes sedimentation time (Fig. 4a). On the other hand, the average hydrodynamic particle sizes were 1240, 1421, 1330 and 1265 nm for 0 mM, 10 mM, 100 mM and 500 mM addition of NaCl, respectively (Fig. 4b). The decreasing trend of the absorbance of ZnO indicated the settlement of ZnO NPs with the increasing of NaCl concentration. However, there was no significant enhancement in the aggregation behavior showed in DLS result when the addition of NaCl concentration increased up to 500 mM, which was consistent with the result of absorbance change and the slightly suppression on degradation rate constants. The dual effect of NaCl on photodegradation was observed by Liu et al. [35]. Chloride ions could enhance or suppress the degradation of acid orange 7 in different systems [36]. The higher NaCl concentration (>50 g/L) is beneficial to increase the amount of reactive chlorine species, while the dye photodegradation rate decreased with low NaCl concentration (<10 g/L), signifying that the concentration impacts the effect of NaCl on the photodegradation [37].

3.4 The effect of sodium bromide on photodegradation of BPA

Experiments of different NaBr concentration on the photocatalytic degradation performances of ZnO on BPA was carried out and shown in Fig. 5a. Upon addition of NaBr from 10 mM to 500 mM concentration in the reaction, the degradation of BPA was found to be suppressing, suggesting a reaction constraining effect. This inhibition could be due to the competition between BPA molecules and bromide ions on the active sites of the catalysts. The photogenerated rate constants were 0.089, 0.0076, 0.0053 and 0.0038 min⁻¹ for 0 mM, 10 mM, 100 mM and 500 mM NaBr addition, respectively (Fig. 5b). The suppression effect of NaBr on BPA degradation was noticeably seen, which was in the following sequence 10 mM>100mM>500mM with almost similar rate constant. In order to observe the hydrodynamic changes of the ZnO NPS, which may affect the surface area and active sites, the DLS study was conducted. The results clearly showed the increase of the average hydrodynamic size of ZnO NPs after the addition of

NaBr. The sedimentation curve of solution indicates the aggregation of ZnO NPs, which could be the reason for the suppression of BPA degradation reaction (Fig. 6a). Further, the average hydrodynamic size of ZnO NPs was found to be 1004 nm for 0 mM NaBr, 1935 nm for 10 mM NaBr, 2399 nm for 100 mM NaBr and 1715 nm for 500 mM NaBr (Fig. 6b). These results show that the BPA photodegradation depends on the ion concentration. The presence of NaCl and NaBr also cause the salting-out effect, results in to the insolubility of BPA, hence decrease the photodegradation [38]. García-Espinoza et al. [39] demonstrated the striking effect of halide ions for dye degradation due to halide radical formation. This study of the electrolyte effect (usually negative) over BPA photodegradation is found to be supporting the degradation process (in the presence of NaCl), by ZnO NPs, hence providing a novel platform for better understanding of the electrolyte-based wastewater treatment.

4. Conclusions

The photodegradation kinetic rate constant of BPA increased with the increase of ZnO dosages from 0.01 to 0.1 g/L, with insignificant adsorption during 30 minutes dark experiment. An obvious aggregation was observed after aqueous dispersion of ZnO NPs, leading to formation of large particles, contrary to the commercial 20 nm particle size. The effect of halide ions during photocatalytic degradation of BPA was investigated using NaCl and NaBr salt solutions. NaBr salt solution restrict the BPA degradation due to aggregation and limited light adsorption capacity. The average hydrodynamic particle size of ZnO NPs increased around 139 %, leading to reduced rate of BPA up to 90 % compared to the one without NaBr. However, NaCl could slightly suppress the degradation rate of BPA around 50 % by 500 mM NaCl. The sedimentation curve reveals no significant change on the particle size and light absorbance efficiency, suggesting the relation between the rate constant and the average hydrodynamic particle size. Suppressed rate of BPA could be anticipated due to competition between NaCl salt and BPA molecules. This study reveals the impact of NaCl and NaBr salt solution on BPA removal and provides an essential information to facilitate the remediation of electrolyte-included wastewater in the future.

Declarations

Ethics declarations

Conflict of interest: The authors declare that they have no conflict of interest.

Ethical approval and consent to participate: Not applicable.

Consent for publication: Not applicable.

Availability of data and materials: All data and materials are included in the manuscript.

Competing interests: No competition interest.

Funding: This research work is financially supported by Ministry of Science and Technology in Taiwan (MOST grant No. 106-2221-E-002-043-MY3).

Author information:

Yi-Chen Yang: Conducted experiment, analyze data.

Rama Shanker Sahu: Design experiments, analyzed data, and wrote the manuscript.

Yang-hsin Shih: Conceptualize, design, and corrected the manuscript.

Corresponding author: Yang-hsin Shih

Acknowledgments

The authors gratefully acknowledge the financial support of the National Science Council of Taiwan, R. O. C. We thank the anonymous referees for reviewing this manuscript.

References

- [1] G. Liu, T. Hyötyläinen, J. Falandysz, Toxicology and Environmental Characteristics of emerging pollutants, 2019.
- [2] S.-Q. Yang, Y.-H. Cui, Y.-Y. Liu, Z.-Q. Liu, X.-Y. Li, Electrochemical generation of persulfate and its performance on 4-bromophenol treatment, Separation and Purification Technology, 207 (2018) 461-469.
- [3] S. Chouhan, S.K. Yadav, J. Prakash, S.P. Singh, Effect of Bisphenol A on human health and its degradation by microorganisms: a review, Annals of microbiology, 64 (2014) 13-21.
- [4] C.-C. Lee, C.-Y. Hsieh, C.S. Chen, C.-J. Tien, Emergent contaminants in sediments and fishes from the Tamsui River (Taiwan): Their spatial-temporal distribution and risk to aquatic ecosystems and human health, Environmental Pollution, 258 (2020) 113733.
- [5] Y. Huang, C. Wong, J. Zheng, H. Bouwman, R. Barra, B. Wahlström, L. Neretin, M.H. Wong, Bisphenol A (BPA) in China: a review of sources, environmental levels, and potential human health impacts, Environment international, 42 (2012) 91-99.
- [6] L.G.A. Barboza, S.C. Cunha, C. Monteiro, J.O. Fernandes, L. Guilhermino, Bisphenol A and its analogs in muscle and liver of fish from the North East Atlantic Ocean in relation to microplastic contamination. Exposure and risk to human consumers, Journal of hazardous materials, 393 (2020) 122419.
- [7] A. Li, T. Zhuang, W. Shi, Y. Liang, C. Liao, M. Song, G. Jiang, Serum concentration of bisphenol analogues in pregnant women in China, Science of The Total Environment, 707 (2020) 136100.

- [8] L.F. Angeles, R.A. Mullen, I.J. Huang, C. Wilson, W. Khunjar, H.I. Sirotkin, A.E. McElroy, D.S. Aga, Assessing pharmaceutical removal and reduction in toxicity provided by advanced wastewater treatment systems, *Environmental Science: Water Research & Technology*, 6 (2020) 62-77.
- [9] M. Dükkancı, Sono-photo-Fenton oxidation of bisphenol-A over a LaFeO₃ perovskite catalyst, *Ultrasonics sonochemistry*, 40 (2018) 110-116.
- [10] B. Kaur, N. Dulova, UV-assisted chemical oxidation of antihypertensive losartan in water, *Journal of environmental management*, 261 (2020) 110170.
- [11] L. Gui, H. Jin, Y. Zheng, R. Peng, Y. Luo, P. Yu, Electrochemical Degradation of Bisphenol A Using Different Modified Anodes Based on Titanium in Aqueous Solution, *Int. J. Electrochem. Sci*, 13 (2018) 7141-7156.
- [12] T. Bao, M.M. Dامتie, A. Hosseinzadeh, W. Wei, J. Jin, H.N.P. Vo, J.S. Ye, Y. Liu, X.F. Wang, Z.M. Yu, Bentonite-supported nano zero-valent iron composite as a green catalyst for bisphenol A degradation: Preparation, performance, and mechanism of action, *Journal of environmental management*, 260 (2020) 110105.
- [13] F.Y. Garcia-Becerra, I. Ortiz, Biodegradation of emerging organic micropollutants in nonconventional biological wastewater treatment: a critical review, *Environmental Engineering Science*, 35 (2018) 1012-1036.
- [14] J.H. Lee, S.-Y. Kwak, Rapid adsorption of bisphenol A from wastewater by β -cyclodextrin-functionalized mesoporous magnetic clusters, *Applied Surface Science*, 467 (2019) 178-184.
- [15] A. Chmayssem, S. Taha, D. Hauchard, Scaled-up electrochemical reactor with a fixed bed three-dimensional cathode for electro-Fenton process: application to the treatment of bisphenol A, *Electrochimica Acta*, 225 (2017) 435-442.
- [16] S. Akbari, F. Ghanbari, M. Moradi, Bisphenol A degradation in aqueous solutions by electrogenerated ferrous ion activated ozone, hydrogen peroxide and persulfate: applying low current density for oxidation mechanism, *Chemical Engineering Journal*, 294 (2016) 298-307.
- [17] Y. Matsumura, C. Hosokawa, M. Sasaki-Mori, A. Akahira, K. Fukunaga, T. Ikeuchi, K.-I. Oshiman, T. Tsuchido, Isolation and characterization of novel bisphenol-A-degrading bacteria from soils, *Biocontrol science*, 14 (2009) 161-169.
- [18] B. Mella, J. Benvenuti, R.F. Oliveira, M. Gutterres, Preparation and characterization of activated carbon produced from tannery solid waste applied for tannery wastewater treatment, *Environmental Science and Pollution Research*, 26 (2019) 6811-6817.
- [19] A. Hernández-Abreu, S. Álvarez-Torrellas, V. Águeda, M. Larriba, J. Delgado, P. Calvo, J. García, Enhanced removal of the endocrine disruptor compound Bisphenol A by adsorption onto green-carbon

- materials. Effect of real effluents on the adsorption process, *Journal of environmental management*, 266 (2020) 110604.
- [20] L.A. Mercante, L.E. Iwaki, V.P. Scagion, O.N. Oliveira, L.H. Mattoso, D.S. Correa, Electrochemical Detection of Bisphenol A by Tyrosinase Immobilized on Electrospun Nanofibers Decorated with Gold Nanoparticles, *Electrochem*, 2 (2021) 41-49.
- [21] C.M. Park, J. Heo, Y. Yoon, Oxidative degradation of bisphenol A and 17 α -ethinyl estradiol by Fenton-like activity of silver nanoparticles in aqueous solution, *Chemosphere*, 168 (2017) 617-622.
- [22] S. Krajangpan, L. Jarabek, J. Jepperson, B. Chisholm, A. Bezbaruah, Polymer modified iron nanoparticles for environmental remediation, *Polym. Prepr*, 49 (2008) 921.
- [23] C.B. Ong, L.Y. Ng, A.W. Mohammad, A review of ZnO nanoparticles as solar photocatalysts: synthesis, mechanisms and applications, *Renewable and Sustainable Energy Reviews*, 81 (2018) 536-551.
- [24] I. Kazeminezhad, A. Sadollahkhani, Influence of pH on the photocatalytic activity of ZnO nanoparticles, *Journal of Materials Science: Materials in Electronics*, 27 (2016) 4206-4215.
- [25] K.M. Lee, C.W. Lai, K.S. Ngai, J.C. Juan, Recent developments of zinc oxide based photocatalyst in water treatment technology: a review, *Water research*, 88 (2016) 428-448.
- [26] P.S. Deokar, L. Cremaschi, Effect of nanoparticle additives on the refrigerant and lubricant mixtures heat transfer coefficient during in-tube single-phase heating and two-phase flow boiling, *International Journal of Refrigeration*, 110 (2020) 142-152.
- [27] K. Choi, T. Kang, S.-G. Oh, Preparation of disk shaped ZnO particles using surfactant and their PL properties, *Materials Letters*, 75 (2012) 240-243.
- [28] R.S. Sahu, Y.-h. Shih, W.-L. Chen, New insights of metal free 2D graphitic carbon nitride for photocatalytic degradation of bisphenol A, *Journal of Hazardous Materials*, 402 (2021) 123509.
- [29] L.V. Trandafilović, D.J. Jovanović, X. Zhang, S. Ptasińska, M. Dramićanin, Enhanced photocatalytic degradation of methylene blue and methyl orange by ZnO: Eu nanoparticles, *Applied Catalysis B: Environmental*, 203 (2017) 740-752.
- [30] Y. Zeng, N. Guo, X. Xu, Y. Yu, Q. Wang, N. Wang, X. Han, H. Yu, Degradation of bisphenol a using peroxymonosulfate activated by WO₃@ MoS₂/Ag hollow nanotubes photocatalyst, *Chemosphere*, 227 (2019) 589-597.
- [31] Q. Chen, H. Wang, Q. Luan, R. Duan, X. Cao, Y. Fang, D. Ma, R. Guan, X. Hu, Synergetic effects of defects and acid sites of 2D-ZnO photocatalysts on the photocatalytic performance, *Journal of hazardous materials*, 385 (2020) 121527.

- [32] R. Saffari, Z. Shariatnia, M. Jourshabani, Synthesis and photocatalytic degradation activities of phosphorus containing ZnO microparticles under visible light irradiation for water treatment applications, *Environmental Pollution*, 259 (2020) 113902.
- [33] R.A. French, A.R. Jacobson, B. Kim, S.L. Isley, R.L. Penn, P.C. Baveye, Influence of ionic strength, pH, and cation valence on aggregation kinetics of titanium dioxide nanoparticles, *Environmental science & technology*, 43 (2009) 1354-1359.
- [34] J. Fatissou, R.F. Domingos, K.J. Wilkinson, N. Tufenkji, Deposition of TiO₂ nanoparticles onto silica measured using a quartz crystal microbalance with dissipation monitoring, *Langmuir*, 25 (2009) 6062-6069.
- [35] W. Liu, Q. Yang, Z. Wang, X. Lv, Z. Yang, Photocatalytic degradation of trichloroethylene over BiOCl under UV irradiation, *Applied Organometallic Chemistry*, 32 (2018) e4354.
- [36] P. Wang, S. Yang, L. Shan, R. Niu, X. Shao, Involvements of chloride ion in decolorization of Acid Orange 7 by activated peroxydisulfate or peroxymonosulfate oxidation, *Journal of environmental sciences*, 23 (2011) 1799-1807.
- [37] J. Qu, R. Chen, X. Dong, J. He, Effect of NaCl concentrations on the photodecoloration of reactive azo-dyes and their cotton dyeings, *Textile Research Journal*, 84 (2014) 2140-2148.
- [38] I. Bautista-Toledo, M.A. Ferro-García, J. Rivera-Utrilla, C. Moreno-Castilla, F.J. Vegas Fernández, Bisphenol A Removal from Water by Activated Carbon. Effects of Carbon Characteristics and Solution Chemistry, *Environmental Science & Technology*, 39 (2005) 6246-6250.
- [39] J.D. García-Espinoza, M. Zolfaghari, P. Mijaylova Nacheva, Synergistic effect between ultraviolet irradiation and electrochemical oxidation for removal of humic acids and pharmaceuticals, *Water and Environment Journal*, 34 (2020) 232-246.

Tables

Table 1. Effect of NaCl and NaBr dosages (mM), observed rate constant (min^{-1}), DLS particle size (nm), and the final pH after certain loading.

	Salt dosage (mM)	Kinetic constant (min ⁻¹)	Final particle size (nm)	Final pH
NaCl	0	0.089	1240	6.70
	10	0.046	1421	6.95
	100	0.038	1330	7.2
	500	0.032	1265	7.45
NaBr	0	0.089	1240	6.45
	10	0.0076	1935	6.75
	100	0.0053	2399	6.98
	500	0.0038	2115	6.85

Figures

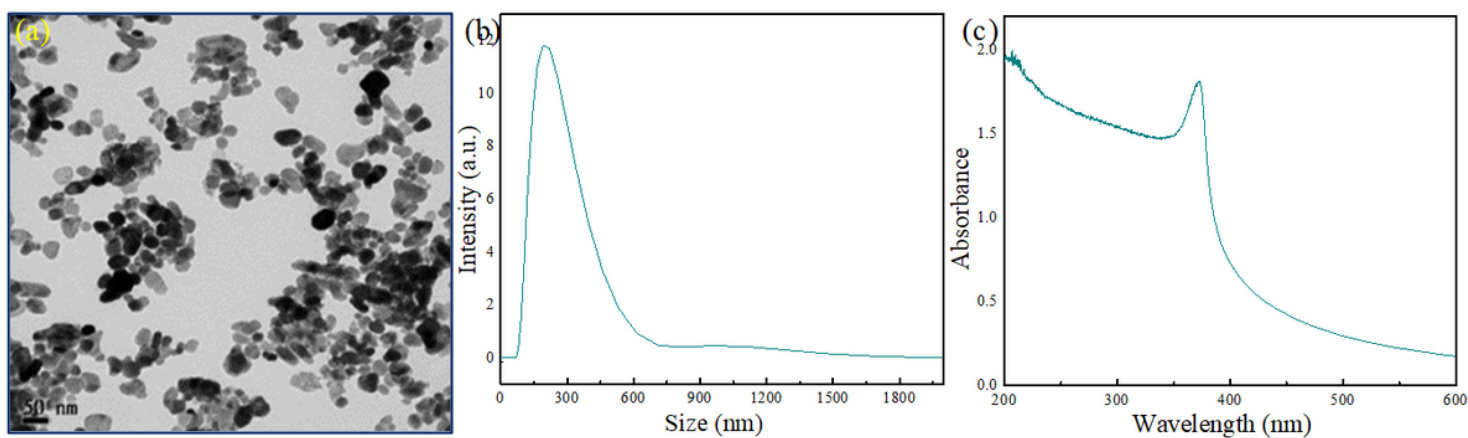


Figure 1

(a) The TEM image, (b) DLS size distribution, and (c) full scan UV-visible spectra of ZnO NPs.

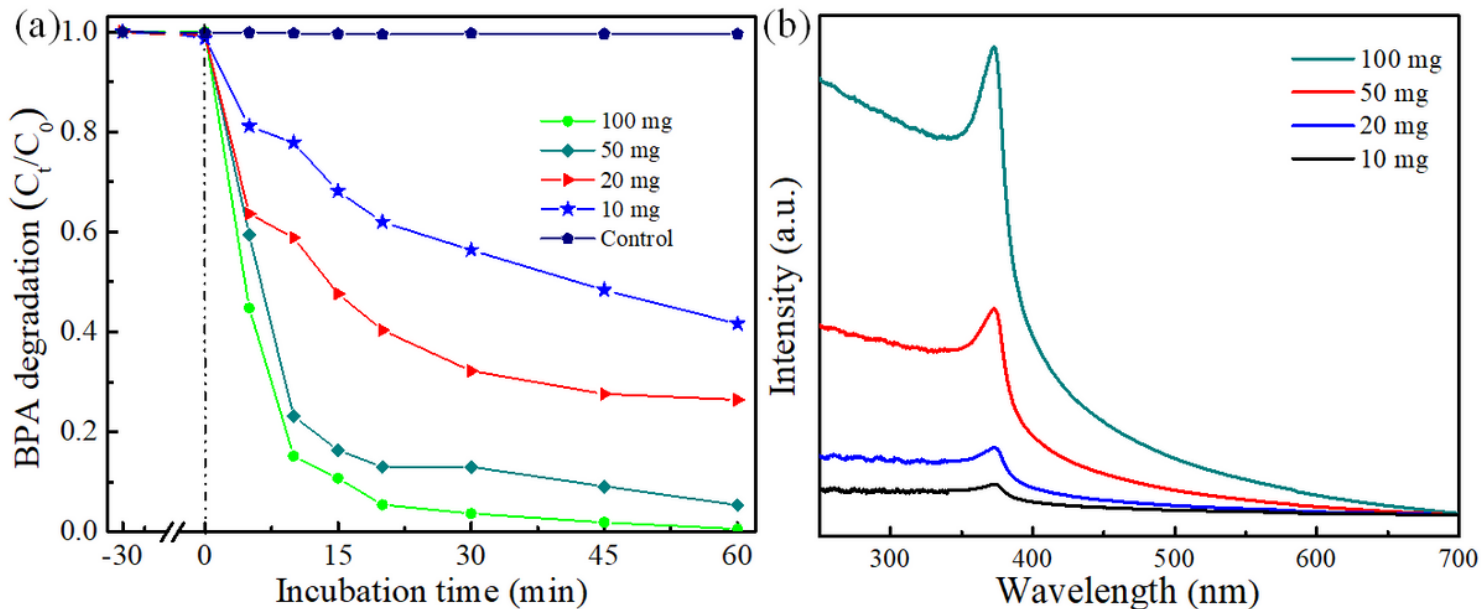


Figure 2

(a) Effect of the initial ZnO catalyst loading on the photodegradation of BPA under 365 nm UV light, (b) full scan UV-visible spectra after different ZnO loading.

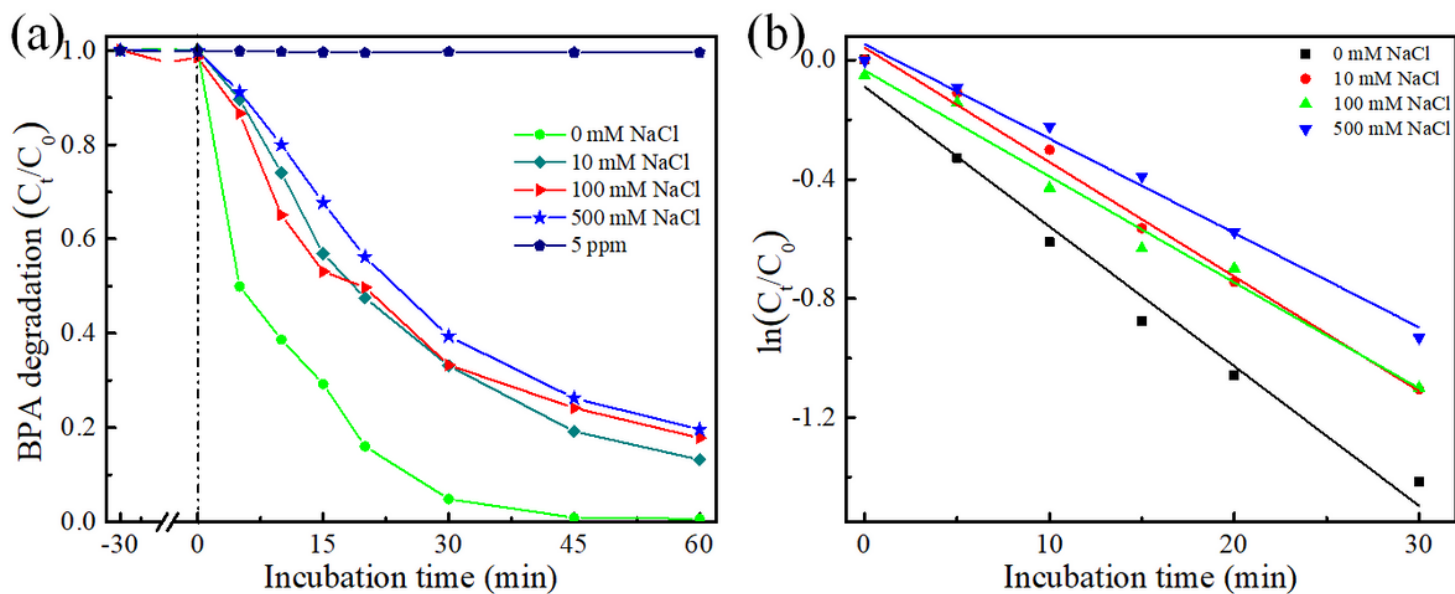


Figure 3

(a) Effect of the NaCl concentration on the photodegradation of BPA under 365 nm UV light, (b) observed rate constant.

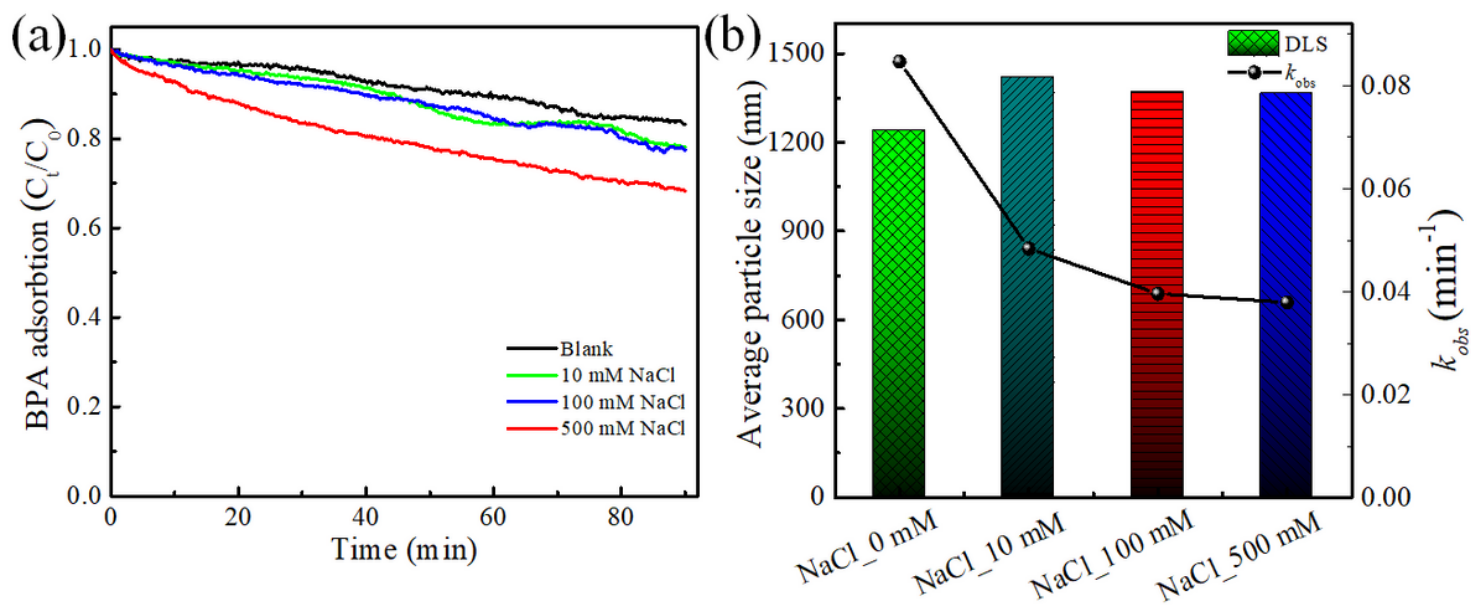


Figure 4

(a) Sedimentation curve after loading different NaCl concentration, (b) effect of NaCl on DLS particle size distribution and rate observed.

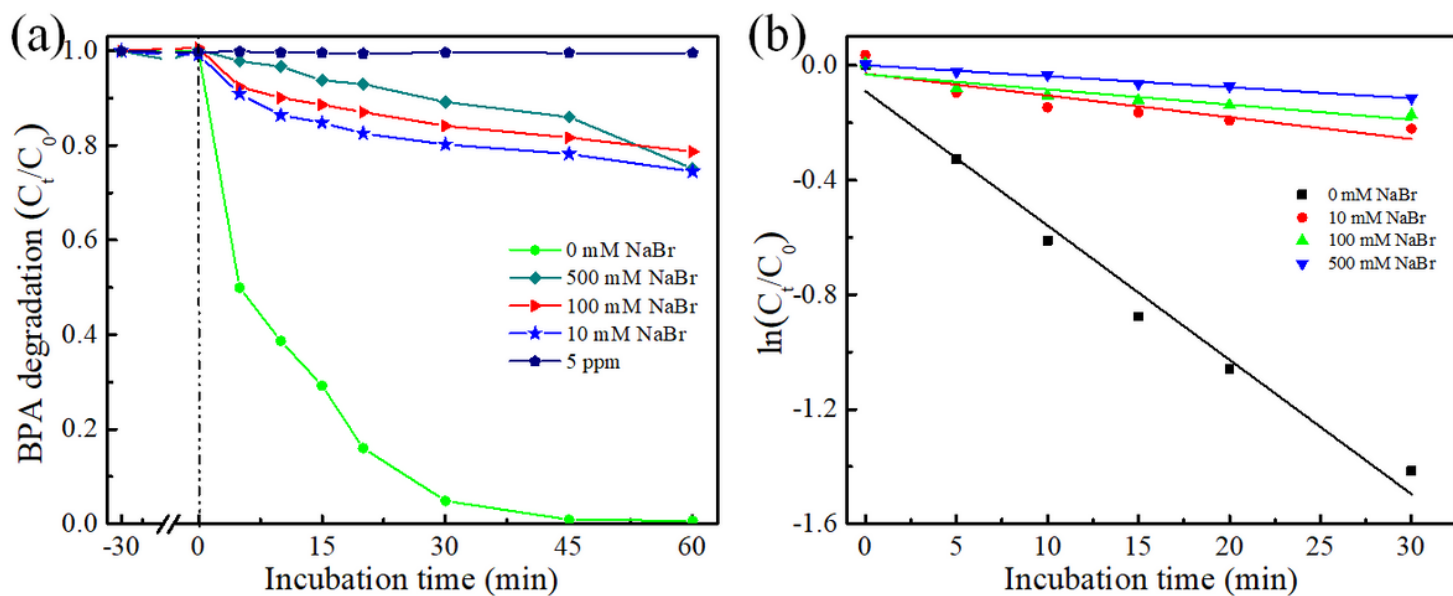


Figure 5

(a) Effect of the NaBr concentration on the photodegradation of BPA under 365 nm UV light, (b) observed rate constant

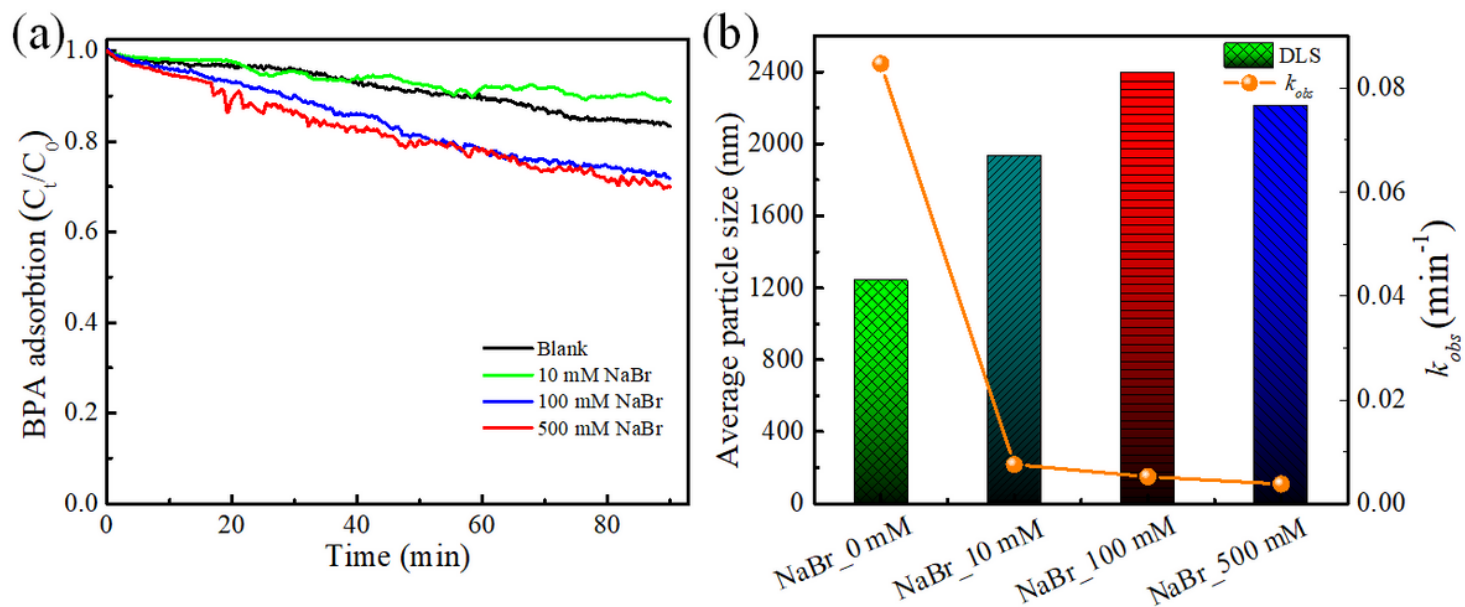


Figure 6

(a) Sedimentation curve after loading different NaBr concentration, (b) effect of NaBr loading on DLS particle size distribution and rate observed.

Supplementary Files

This is a list of supplementary files associated with this preprint. Click to download.

- [Graphicalabstract.docx](#)